Twinned Crystal Structure And Characterization Of [Cu(Hseo$_3$)$_2$Cu$_{0.34}$Se$_{0.58}$Cl$_3$(H$_2$O)$_3$]

H. Belgaroui[a], M. Loukil[a], A. Kabadou[a] , H. Khemakhem[b] and A. Ben Salah[a]

[a] Laboratoire des Sciences des Matériaux et d'Environnement, Faculté des Sciences de Sfax – Tunisie
[b] Laboratoire des Matériaux Ferroélectriques, Faculté des Sciences de Sfax, B.P. 802, 3018 Sfax, Tunisie

Abstract:

The structure of a newly layered copper selenium hydrogenselenite [Cu(HSeO$_3$)$_2$Cu$_{0.34}$Se$_{0.58}$Cl$_3$(H$_2$O)$_3$] has been solved from single crystal X-Ray diffraction data and refined to a final reliability factor R_1= 0.0338 . It was found having an orthorhombic space group Pbn2$_1$, with a = 7.1753(4) Å, b=9.0743(4)Å, c=17.7246(9) Å, V = 1154.06(9) Å^3, and Z = 4. This structure is three-dimensional but it may be described as a bidimensional structure made of layers, parallel to the (010) plane, which contain copper atoms and (HSeO$_3$)$^-$ anions. The sheets are interconnected by [CuCl$_3$(H$_2$O)$_3$] groups. The Se and Cu oxidation state was evaluated using bond valence sum calculations.

The presence of hydrogenoselenites (νSe-O-H, 1222cm^{-1}) was confirmed by IR and Raman spectra. The dielectric constant at different frequencies and temperatures revealed a phase transition at 383 K.

Keywords: Bimetallic hydrogenselenites, Dielectric properties, Structural study.

1. Introduction

Within the last years, research in hydrogenselenite chemistry has been mostly driven by the motivation to expand the knowledge of structural and bonding principles in this ligand. An important number of crystal structures of divalent metal hydrogenselenites has been reported : M(HSeO$_3$)$_2$ (where M: Cu, Mg, Sr, Ba) [1,2]; M(HSeO$_3$)$_2$.H$_2$O (where M: Ca, Cu) [3–6]; M(HSeO$_3$)$_2$.NH$_4$Cl (where M: Cu) [7]; [Cu(HSeO$_3$)$_2$Cu$_x$M$_{1-x}$Cl$_2$(H$_2$O)$_4$] with M = Cu, Co, Mn, Ni and Zn [8]. This family has a three-dimensional structure but it may be considered as being derived from the [Cu(HSeO$_3$)$_2$] type structure.

Compounds exhibiting mixed valences are subject to many studies because of their potential applications related to the electronic exchange. Magnetic measurements reveal the occurrence of weak ferromagnetism at low temperature (T= ~ 10-20 K) for almost all compounds except [Cu(HSeO$_3$)$_2$]. A tentative explanation will be offered for this peculiar property [8,9].

To complete this study, we present here the crystal structure analysis obtained from X Ray single structure, spectroscopy characterization and dielectric measurements for [Cu(HSeO$_3$)$_2$Cu$_{0.34}$Se$_{0.58}$Cl$_3$(H$_2$O)$_3$] compound.

2. Experimental
2. 1. Synthesis

The experiments were carried out using a single crystal of [Cu(HSeO$_3$)$_2$Cu$_{0.34}$Se$_{0.58}$Cl$_3$(H$_2$O)$_3$] grown by slow evaporation from a mixture of hydrochloride acid containing stoechiometric CuCl$_2$–SeO$_2$ at room temperature in the ratio   1/ 2. Blue thin rectangular parallelepiped crystals were grown after vaporizing in air for 15 days approximately.

2.2. Characterization

The [Cu(HSeO$_3$)$_2$Cu$_{0.34}$Se$_{0.58}$Cl$_3$(H$_2$O)$_3$] formula was determined by the crystal structure refinement at room temperature.

Electrical impedances measurements were realized in the range [1–10] KHz using a Hewlett-Packard 4192 ALF automatic bridge monitored by a HP vectra microcomputer. Dense translucent pellets (8 mm in diameter, 1–1.2 mm in thickness) were used for measurements. The pellet was covered with graphite electrodes.

Infrared absorption spectrum of suspensions of crystalline powders in KBr was recorded on a Perkin-Elmer 1750 spectrophotometer IR-470 in the range 400–4000 cm^{-1}.

The Raman spectrum was recorded at room temperature on a Horibo Jobin Yvan HR800 microcomputer system instrument using a conventional scanning Raman instrument equipped with a Spex 1403 double monochromator (with a pair of 600 grooves/mm gratings) and a Hamamatsu 928 photomultiplier detector. The excitation radiation was provided by coherent radiation with an He-Neon laser at a wavelength of 633 nm, and the output laser power was 50 mW. The spectral resolution, in terms of slit width, varied from 3 to 1 cm^{-1}.

2.3. Crystal data of [Cu(HSeO$_3$)$_2$Cu$_{0.34}$Se$_{0.58}$Cl$_3$(H$_2$O)$_3$]

The crystal structure of $[Cu(HSeO_3)_2Cu_{0.34}Se_{0.58}Cl_3(H_2O)_3]$ was studied using an APEX II diffractometer with graphite–crystal monochromated Mo Kα radiation (0.71073 Å). A total of 3093 reflections were collected, among which only 2803 reflections, namely those for which $I > 2\sigma (I)$, were used to determine and refine the structure. Corrections were made for Lorentz–Polarisation and absorption effects. Data collection procedure and structure refinement at room temperature, are given in Table 1. The selenium atoms positions were determined using a three dimensional Patterson synthesis. Chlorine, copper and oxygen atoms were located by three-dimensional Fourier function. Hydrogen atoms were localized from a difference Fourier synthesis. All the non-hydrogen atoms were assigned anisotropic thermal displacements. $[Cu(HSeO_3)_2Cu_{0.34}Se_{0.58}Cl_3(H_2O)_3]$ crystallizes with orthorhombic symmetry ($Pbn2_1$ space group). The density measured by helium picnometry ($\square$ exp = 3.08 g/cm^3) implies Z = 8 $[Cu(HSeO_3)_2Cu_{0.34}Se_{0.58}Cl_3(H_2O)_3]$ per unit cell ($\square$ calc =3.149 g/cm^3). The structure was solved by patterson method using the SHELXS 86 program [10]. The atomic coordinates and anisotropic thermal parameters for all atoms were refined using the SHELXL-97 program [11].

The structure of $[Cu(HSeO_3)_2Cu_{0.34}Se_{0.58}Cl_3(H_2O)_3]$ was refined by assuming the above mentioned non-centrosymmetric space group, undertaking and evaluating the absolute-structure. The values of the Flack parameter x [12] and its standard uncertainty u were equal to 0.52 and 0.02, respectively. From the full text of Flack and Bernardinelli [13], it was deduced that the value of u = 0.02 indicates a strong inversion-distinguishing power, and that the domains around the value of x should be well defined and clearly distinguishable from one another.

Such a parameter value indicates that the crystal is twinned by inversion. Consequently, it should be considered as constituted by a mixture of domains with inverted structures, and its absolute structure determination is not possible. A final refinement taking into account these domains by way of the TWIN/BASF instructions as recommended by SHELXL-97 program converged to final reliability factors R1 = 0.0338 and wR2 = 0.0878

The refined atomic coordinates and anisotropic displacement parameters are presented in Tables 2 and 3. Table 4 reports the main interatomic distances and angles. DIAMOND program was used for graphical representations [14].

3. Results and discussion
3.1 Structure description
3.1.1 Bond Valence

The charge balance in $[Cu(HSeO_3)_2Cu_{0.34}Se_{0.58}Cl_3(H_2O)_3]$ suggests that the average oxidation state of Cu(2)/Se(2) is equal to 3, which would fit to 34 of Cu^{2+} and 58% of Se^{4+}. To confirm this consequence, a calculation of bond valence sums around the centers of the cation sites was done.

The bond valence (S_{ij}) is given by S_{ij}= exp $[(R_0- R_{ij})/B]$ where R_0 and B are the experimentally determined parameters and R_{ij} is the bond length of the cation − anion pair [15]. Based on the valence sum rule, the sum of the bond valence ($\sum_j S_{ij}$) around an ion must be equal to the formal valence (V_i) of this ion.
Our calculation shows that for the pyramidal sites (Se1 and Se3), sum of bond valence is approximately 4, is equal to selenium formal valence.
Bond valence sums around the octahedral site of Cu(2) is consistent with the value +2.7 which confirm the presence of selenium Se^{4+} and copper Cu^{2+} in the same site.

3.1.2 Structure determination
The blue single crystal $[Cu(HSeO_3)_2Cu_{0.34}Se_{0.58}Cl_3(H_2O)_3]$ crystallizes in the orthorhombic system with space group $Pbn2_1$.
The crystal structure of $[Cu(HSeO_3)_2Cu_{0.34}Se_{0.58}Cl_3(H_2O)_3]$ represents a new type of structure for complexes hydrogenselenites (Figure1). The building blocs $[Cu_{0.34}Se_{0.58}(HSeO_3)_2]$ and $[CuCl_3(H_2O)_3]$ are arranged to form layers in the structure parallel to the (010) plane between which the lone pairs E are located (Figure.2).
Due to the stereochemical activity of the lone pairs E, Se has very asymmetric coordination polyhedra SeO_3 pyramids.

3.1.2.1 Environment of copper cations Cu(1)
Each Cu(1) atom is surrounded by three oxygen atoms and three chlorine atoms forming a slightly distorted octahedron with distances ranging from 1.99(7) to 2.21(3) Å for Cu-O and 2.30 (2) Å for Cu-Cl (Figure.4).

3.1.2.2 Environment of copper/selenium cations Cu(2)/Se(2)
During refinement, the occupancy of the Cu(2) site exhibited a significant deviation from full occupancy, indicating a substitution with Se; the final occupancies were constrained to sum to 1.0 and refined to 0.37 and 0.63, respectively, for Cu(2) and Se(2).
The Cu(2)/Se(2) atoms are surrounded by four oxygen atoms and two chlorine atoms form an irregular octahedron (Figure.5).

3.1.2.3 Environment of selenium cations
For the Se1 and Se3 atoms, the distribution of anions around each cation is highly anisotropic

and characteristic of a strong stereochemical activity of their electron lone pair E. The coordination polyhedral can be described as a distorted SeO_3 triangular pyramid, with the Se-O(7) and Se-O(8) marginally longer than the other Se-O bonds (Table 4), and with the lone pair E so directed to constitute the fourth vertex of a SeO_3E tetrahedron (Figure.3.). The Se–O chemical bonds, forming O–Se–O angles of values 98(2)° and 102(2)°, are situated on one side of the Se atom, whereas the other side is a 'dead' zone around the lone pair E of the Se atom. Due to such a sharp asymmetry of the atomic arrangement of the first coordination spheres, the SeO_3 polyhedra have strong dipole moments which provide considerable dipole-dipole contribution to the inter-anion potentials.

The structure represented in Figure.2 is formed by Cu(1), Se(2)/Cu((2) polyhedra sharing chlorine corners in infinite chains along the direction [001]. The sequence of metal atoms in the chain follows the scheme Cu(1)–Se(2)/Cu(2)– Cu(1)'–Se(2)/Cu(2)–Cu(1) , where the prime refer to the polyhedra generated by the symmetry operation: 1-x, 2-y, -0.5+z, in the [010] direction, thus forming a three-dimensional network.

The lattice cohesion is strengthened by hydrogen bonds within the layer (O(8)-H(7)-O(4)) and (O(7)-H(8)-O(3)) or outside the layer (Table 5).

3.2 Spectroscopic studies

IR and Raman spectroscopy were used to confirm the crystallographic results of $[Cu(HSeO_3)_2Cu_{0.34}Se_{0.58}Cl_3(H_2O)_3]$ compound.

The IR spectrum is restricted to the frequency range: 400 to 4000 cm^{-1} (Figure.6).

3.2.1. HSeO₃ vibrations

Vibrational analysis on a series of alkali hydrogen selenites by Cody and al. and Micka and al., shows that the symmetric stretching vibrations are around 850 cm^{-1} [16-18]. In the present work, the band corresponding to the symmetric stretching vibrations of SeO_2 groups is obtained at around 825 cm^{-1} of the Raman spectrum (Figure.7). A strong intense band broad is observed in the infrared spectrum for this mode.

The asymmetric stretching vibrations of SeO_2 groups are observed as band of weak intensity at 710 cm^{-1} accompagned by a shoulder at 738 cm^{-1}. Corresponding IR spectrum gives an intense broad band in the 686-740 cm^{-1} region. These modes are observed at lower wavenumbers than those in alkali hydrogen selenites [19,20].

The copper (selenium) atoms are located at the centre of $CuCl_2O_4$ coordination octahedra. The axial Cu-Cl bonds are longer than the others and they are coordinated to water molecules. The high spin d-configuration of Cu leads to Jahn-Teller distortions to produce planar Cu-O bonds in the 1.91-1.98 Å range and an axial Cu-Cl distance of 2.77-2.80 Å. The fact that the planar oxygen atoms are shared by Cu and Se atoms can lead to the observed reduction in the stretching frequencies of the SeO_2 groups.

The stretching vibrations of the $HSeO_3^-$ ion (νSe-OH), usually observed in the 600-650 cm^{-1} region, are also obtained at lower wave numbers (~627cm^{-1}). This mode is observed as an intense broad band at 532 cm^{-1} in the IR spectrum. The O •. • O distance involving the Se-OH system with one of the equatorial oxygen atoms of the neighbouring $Cu(2)/Se(2)Cl_2O_4$group is 2.662 Å. The observed lowering of the Se-O(H) vibrations from the free state values is a confirmation of the corresponding strong hydrogen bonds predicted in the X-ray diffraction data. Symmetric deformation vibrations of the $HSeO_3^-$ ion (Table 6) give only weak bands of the Raman spectrum while a medium intense broad band is obtained in the IR. In the asymmetric bending vibration, Raman spectrum shows medium intense bands with a weak band in the IR. A reduction in the symmetry of the $HSeO_3^-$ ion causes the changes in the activity of these modes.

It is to be noted that all bands, both stretching and bending, appear broad in both the IR and Raman spectra. This is consistent with the strong hydrogen bonding and the distortion of $Cu(Se)O_4Cl_2$ octahedra due to the Jahn-Teller effect which also affect the $HSeO_3$ vibrations.

3.2.2. Hydrogen bond and water vibrations

Hydrogen bonded OH groups lead to three fundamental vibrations, the ν(OH) stretching and the in-plane δ(OH) and the out-of-plane γ(OH) deformation vibrations. The stretching bands of strongly hydrogen bonded systems are very broad and are built up of a number of unresolved components due to strong interaction between the proton vibration and the ν(O . . . O) vibrations [21,22]. The broad ν(OH) band in Fermi resonance with the overtones of the δ(OH) the γ(OH) modes splits into three bands A, B and C [23,24]. The A mode is observed as a strong broad band at 2850 cm^{-1} in the IR spectrum while the B mode is obtained as a medium intense band at 2360 cm^{-1}. A medium intense broad band at 1900 cm^{-1} and a weak one at 1730 cm^{-1} are assigned to C bands. The appearance of these bands confirms the existence of strong hydrogen bonds in the crystal.

The in-plane bending δ(OH) vibrations are less sensitive to the hydrogen bond strength than the γ(OH) mode [18]. A medium band observed at 1280 cm^{-1} in the IR spectrum is attributed to the in-plane γ(OH) bending mode and a medium intense broad band in the 870-940 cm^{-1} region to the γ(OH) mode.

Two broad bands are observed in the stretching region of water in the Raman spectra of the title compound. In the IR spectrum, a strong

broad band with two distinct peaks at 3553 and 3170 cm^{-1} are obtained for this mode. The bending mode of H_2O appears at around 1606 cm^{-1} in the IR. The considerable shifting of stretching and bending frequencies from those of a free water molecule [25] indicates the presence of strong hydrogen bonding in our crystal.

3.2.3. External modes

The external modes of the $HSeO_3$ ion, lattice modes of water and metal-oxygen stretching modes appear approximately below 200 cm^{-1}.

3.3. Dielectric studies

Figure.8 illustrates the temperature dependence of the dielectric constant (ε') in the frequency range [1–10] KHz and in the temperature region 300-500K for $[Cu(HSeO_3)_2Cu_{0.34}Se_{0.58}Cl_3(H_2O)_3]$. These curves exhibit:

One anomaly in the dielectric constant ε' at about 393 K. The maximum of the permittivity curves decreases with increasing frequency.

Some complex impedance diagrams having $-\varepsilon''$ versus ε' recorded at various temperatures are presented in Fig. 9. As the temperature increases, the semicircles move to a lower value of resistance. So, the complex impedance spectra show that the title compound follows the cole–cole law. The direct conductivity (d.c.) of this material was deduced from the resistance Rp by the relation:

$\sigma = [L/(Rp.S)]$ where L, S and Rp are respectively the thickness, the surface of the pellets and the d.c resistance, which determined by extrapolation of the circular arc to the real axis at low frequency part of the complex impedance plot [26]. The evolution of the direct conductivity (d.c.) versus inverse temperature $\log(\sigma)= f(10^3/T)$ is shown at Fig. 10. This curve exhibits a phase transition at T $\Box$ 393 K. The electrical conductivity increases with increasing temperature in both phases. The change in σ occurs at the transition temperature. The temperature dependence of electrical conductivity measured in both phases is well described by an Arrhenius equation of the form:

$\sigma.T = A \exp(-E_a / k_B T)$; where A is the pre-exponential factor, K_B is the Boltzman constant and Ea is the apparent activation energy for the ion migration.

The activities energies at low and high temperature are $\Box$ E$_{LT}$ = 0.362 eV, $\Box$ E$_{HT}$ = 1.65 eV, respectively.

The transition at T= 393 K is related to a motion of a rapid reorientation of $(HSeO_3)^-$ and H^+ diffusion [27]. However if the temperature increases, the reorientation of the $(HSeO_3)^-$ groups becomes more exited and the proton H^+ can jump over the potential barrier.

4. Conclusion

In conclusion, we have successfully prepared a novel substituted hydrogenoselenites $[Cu(HSeO_3)_2Cu_{0.34}Se_{0.58}Cl_3(H_2O)_3]$ via slow evaporation method. The crystal structure of the title compound is characterized by the presence of blocs $[Cu_{0.34}Se_{0.58}(HSeO_3)_2]$ and $[CuCl_3(H_2O)_3]$ arranged to form layers in the structure parallel to the (001) plane between which the lone pairs E are located . So, the main of the feature structure of this compound is based on different coordination polyhedral, SeO_3 pyramids and $[CuCl_3(H_2O)_3]$ octahedra.

The presence of hydrogenoselenites (νSe-O-H, 1222 cm^{-1}) was confirmed by IR and Raman spectra.

The particularity of $[Cu(HSeO_3)_2Cu_{0.34}Se_{0.58}Cl_3(H_2O)_3]$ is that it undergoes a phase transition on heating at 383 K. High-temperature structure investigation of the title compound is in our future plans in order to confirm the nature of this transformation.

References

[1]. M.Koskenlinna, Valkonen, J Acta Crystallogr C. 51 (1995) 1637.
[2]. M.Z Cermak, Niznansky, Chem.Commun. 55 (1990) 2441.
[3]. K.Unterderweide, B.Engelen, K.Boldt, J. Mol. Struct. 322 (1994) 233.
[4]. K.Boldt, Thesis, (1994) Universita Siegen,.
[5]. J.Valkonen, J. Solid State Chem. 65 (1986) 363.
[6]. L.Hiltunen, M.Leskela, L.Niinisto, M.Tammenmaa, Acta Chem.Scand.A, 39 (1985) 809.
[7]. J.CTrombe , A.M.Lafront, J. Bonvoisin, Inorg. Chim. Acta, 238 (1997) 47.
[8]. A.M.Lafront, J.C.Trombe,J. Bonvoisin, Inorg. Chim. Acta, 238 (1995) 15.
[9]. A.M.Lafront, Thesis, (1995) University of Toulouse.
[10]. G.M.Sheldrick, SHELXS97. Program for the Refinement of Crystal Structures, University of Gottingen, Germany,.
[11]. G.M.Sheldrick, SHELXL97. (1997) Program for the Refinement of Crystal Structures, University of Gottingen, Germany,.
[12]. H.D. Flack, Acta Cryst. A39 (1983) 876–881.
[13]. H.D. Flack, G. Bernardinelli, J. Appl. Cryst. 33 (2000) 1143–1148.
[14]. K. Brandenburg, DIAMOND, Crystal Impact GbR, Version 2.1e, Bonn, Germany, (2001).
[15]. R.D.Shannon, Acta Crystallogr.Sect. A 32 (1976) 751

[16]. C.A.Cody, R.C.Levitt, R.S.Viswanath, P.J.Miller, J. Solid State Chem.26 (1978) 281.

[17]. L.Richtera, J.Taraba, J.Toužín, Z. Anorg. Allg. Chem. 629 (2003) 716

[18]. R.Ratheesh, G.Suresh, M.J.Bushiri, Speetrochimica Acta Part A 51 (1995) 1509

[19]. H.D.Lutz, H.Haeuseler, Journal of Molecular Structure 511 (1999) 69

[20]. M.Tanimizu, Y.Takahashi, M. Nomura, Geochemical Journal 41 (2007) 291

[21]. M.F.Claydon, N.Sheppard, Chem. Phys. (1969) 1431.

[22]. S.Bartos, H.Ratajczak, J. Mol. Struct.76 (1982) 77.

[23]. J.Baran, T.Lis, M.Marchewka, H.Ratajczak, J.Mol. Struct. 250 (1991) 13.

[24]. H.Ratajczak, A.M.Yaremko, J.Baran, J. Mol. Struct., 275 (1992) 235.

[25]. J.T.Kloprogge, R.L.Frost, Applied Spectroscopy Issue 4 54, (2000) 517

[26]. J.E.Bauerele, J.Hrizo, J. Phys. Chem. Solids 30 (1969) 565.

[27]. K. Jaouadia, N. Zouari, T. Mhiri, M. Giorgi, Physics Procedia 2 (2009) 1185–1194

Figure captions

Fig.1. Perspective view of the $[Cu(HSeO_3)_2Cu_{0.34}Se_{0.58}Cl_3(H_2O)_3]$ unit cell content.

Fig.2. A projected along a-axis view of the $[Cu(HSeO_3)_2Cu_{0.34}Se_{0.58}Cl_3(H_2O)_3]$ unit cell content. Observation of a lone pairs E

Fig.3. Environment of selenium Se(1),Se(3) cations.

Fig.4. Environment of cupper cations Cu(1).

Fig.5. Environment of cupper/selenium cations Cu(2)/Se(2).

Fig.6. Infra red spectrum of $[Cu(HSeO_3)_2Cu_{0.34}Se_{0.58}Cl_3(H_2O)_3]$ at room temperature.

Fig.7. Raman spectrum of $[Cu(HSeO_3)_2Cu_{0.34}Se_{0.58}Cl_3(H_2O)_3]$ at room temperature.

Fig.8. Temperature dependence of ε' as a function of frequency for $[Cu(HSeO_3)_2Cu_{0.34}Se_{0.58}Cl_3(H_2O)_3]$

Fig.9. Complex impedance diagrams -Z'' versus Z' for $[Cu(HSeO_3)_2Cu_{0.34}Se_{0.58}Cl_3(H_2O)_3]$ at various temperatures

Fig.10. Conductivity plots log ($\square$) =f (1000/T) for $[Cu(HSeO_3)_2Cu_{0.34}Se_{0.58}Cl_3(H_2O)_3]$
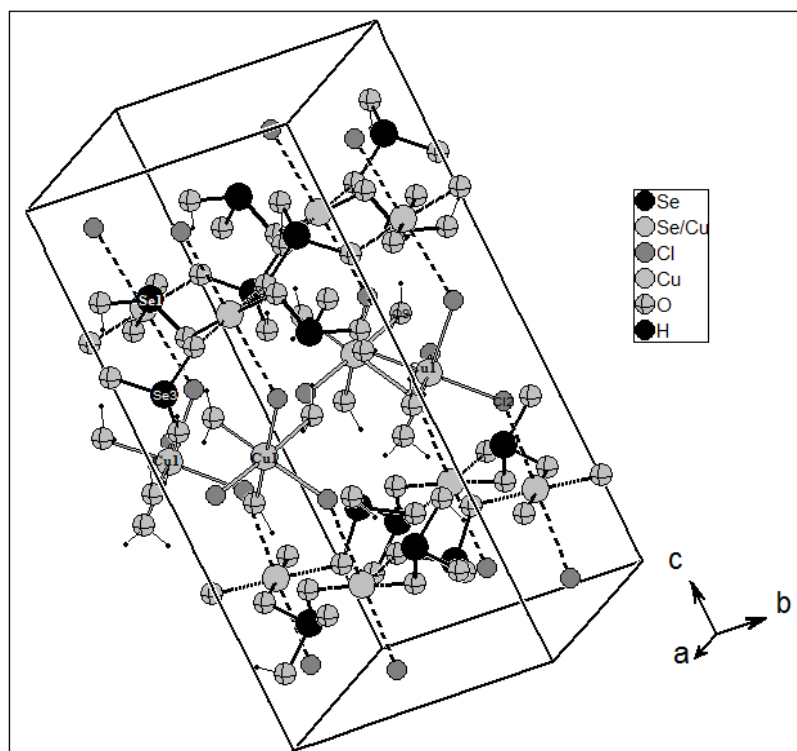
Fig.1
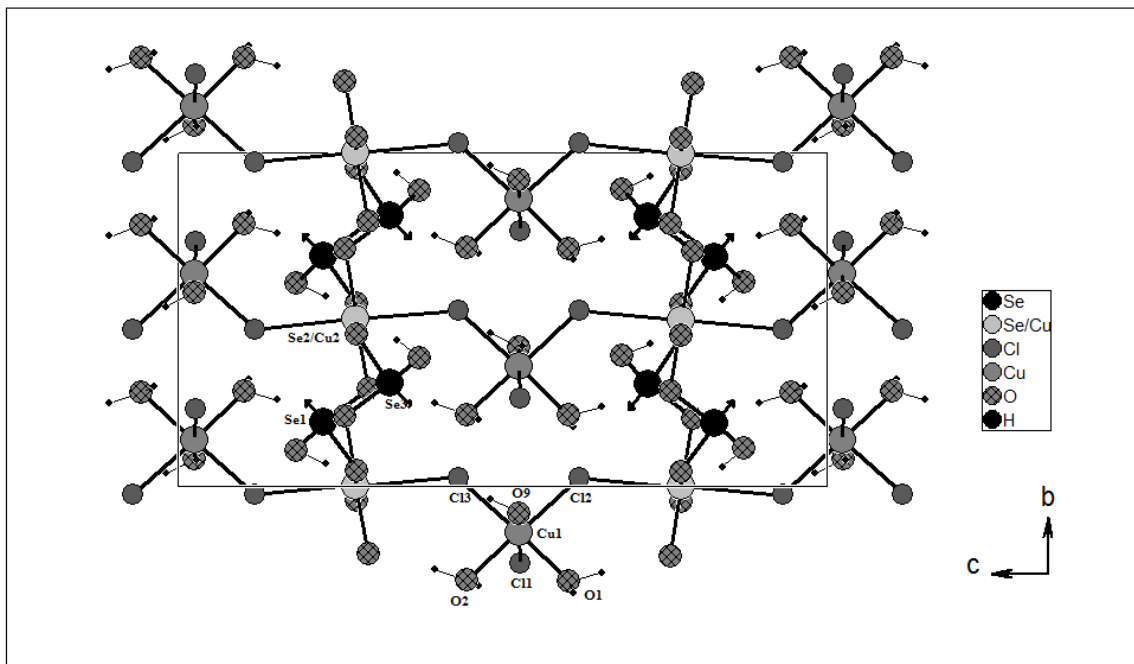
Fig.2
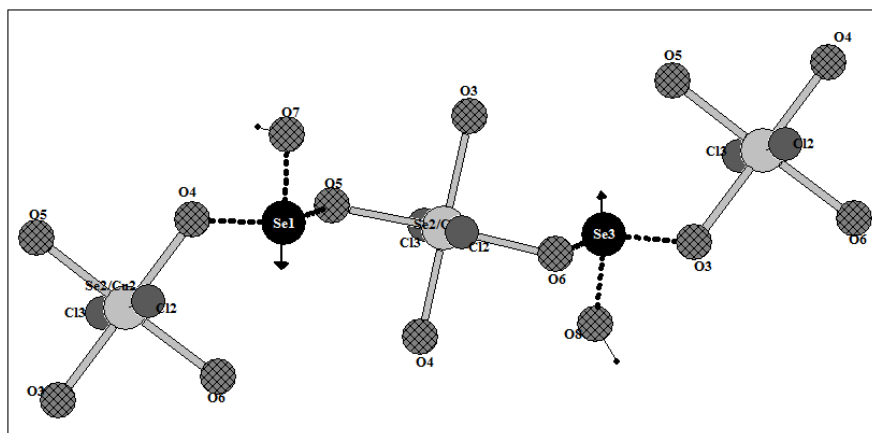
Fig.3
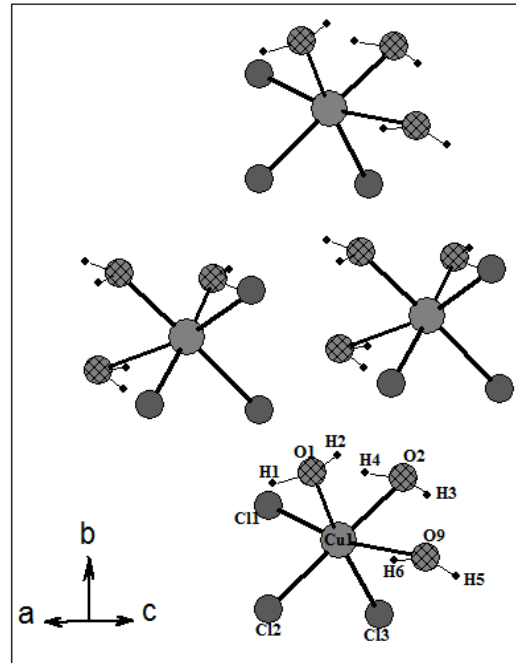
Fig.4
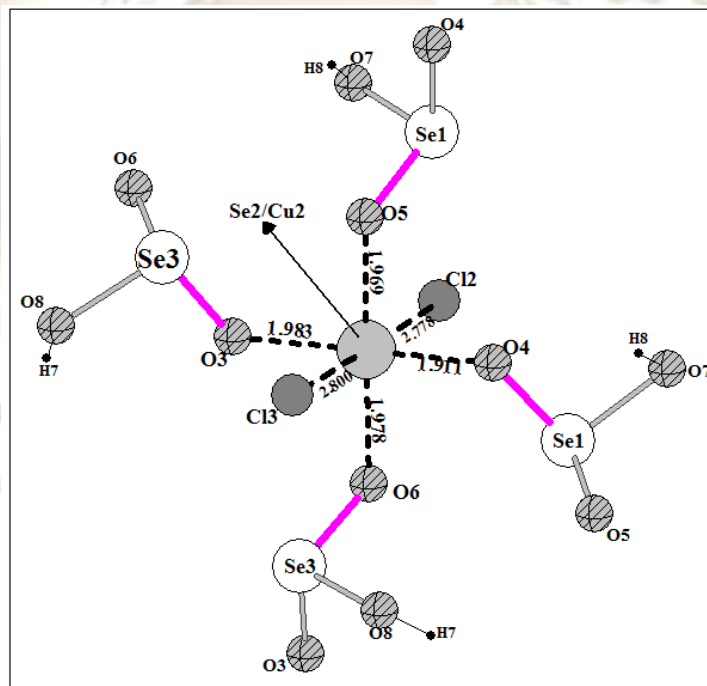
Fig.5
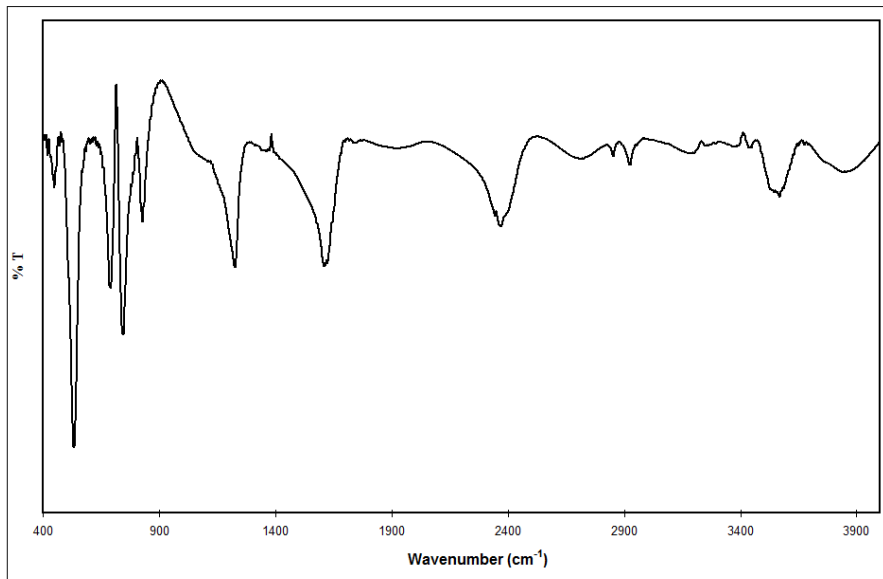
Fig.6
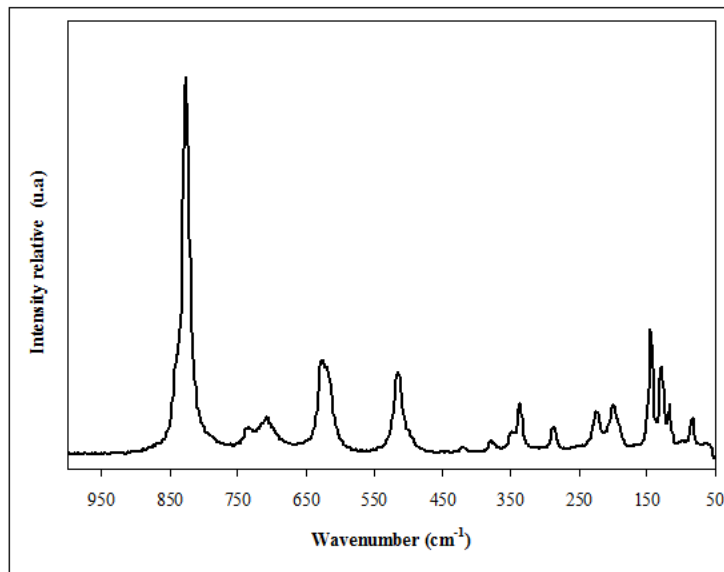
Fig.7
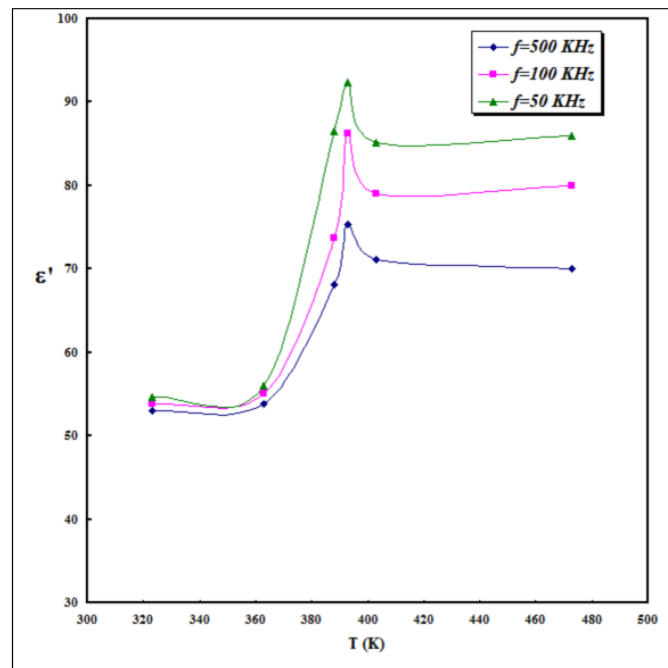
Fig.8
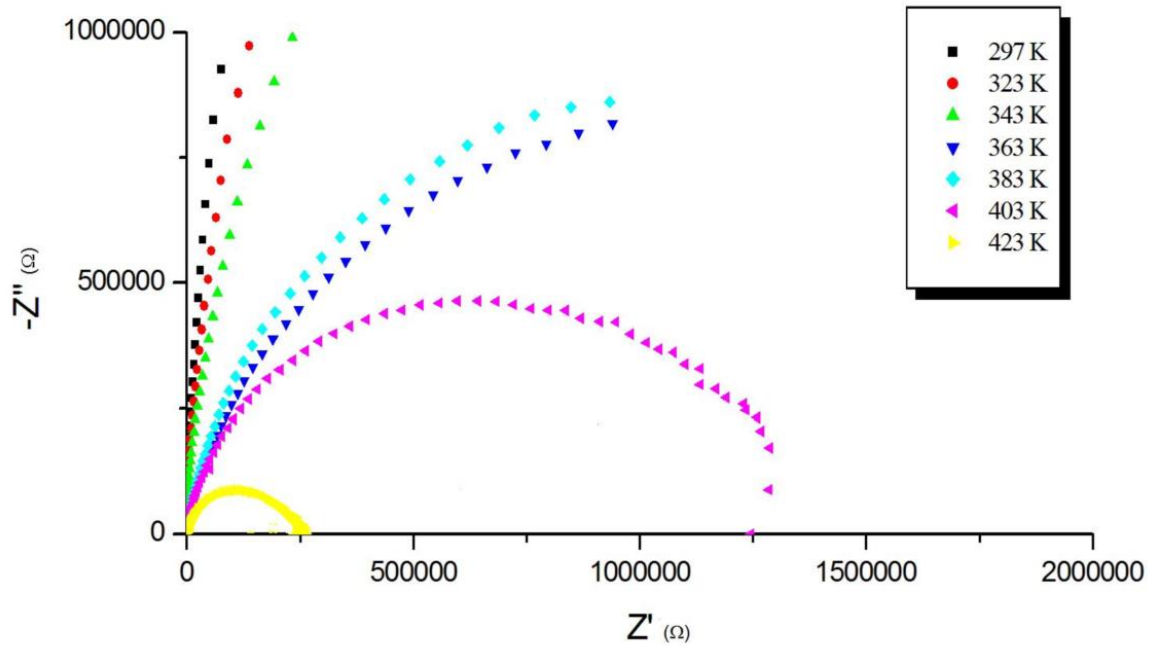
Fig.9
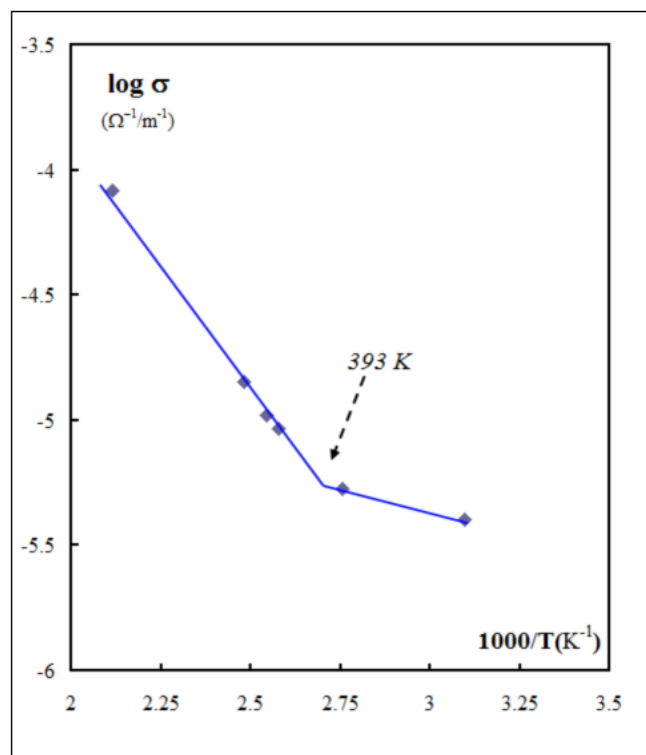
Fig.10

Caption Tables

Table 1.
Crystal structure data and experimental conditions of structure determination of $[Cu(HSeO_3)_2Cu_{0.34}Se_{0.58}Cl_3(H_2O)_3]$

Table 2.
Atomic coordinates and equivalent isotropic displacement parameters (Å^2) for $[Cu(HSeO_3)_2Cu_{0.34}Se_{0.58}Cl_3(H_2O)_3]$

Table 3.
Anisotropic displacement parameters for $[Cu(HSeO_3)_2Cu_{0.34}Se_{0.58}Cl_3(H_2O)_3]$

Table 4.
Interatomic distances for $[Cu(HSeO_3)_2Cu_{0.34}Se_{0.58}Cl_3(H_2O)_3]$ samples.

Table 5.
Hydrogen bonding systems of $[Cu(HSeO_3)_2Cu_{0.34}Se_{0.58}Cl_3(H_2O)_3]$, distances (Å) and angles (°).

Table 6.
Assignment and frequencies (cm^{-1}) observed for IR and Raman spectra of $[Cu(HSeO_3)_2Cu_{0.34}Se_{0.58}Cl_3(H_2O)_3]$ at room temperature.

Table 1.

Formula	$[Cu (HSeO_3)_2 Cu_{0.34}Se_{0.58}Cl_3(H_2O)_3]$
Formula weight	547.15
Space group	$Pbn2_1$
a (Å)	7.1753(4)
b(Å)	9.0743(4)
c(Å)	17.7246(9)
V(Å^3)	1154.06(10)
Z	4
ρ_{calc} (g/cm^3)	3.149
μ (mm^{-1})	11.359
Crystal size (mm^3)	$0.18 \times 0.26 \times 0.47$
Crystal shape	octahedral
F(000)	1030
Data collection instrument	Kappa- APEX II
Radiation, graphite monochromator	$\lambda_{Mo\ K\alpha}$ (0.71073 Å)
θ range for data collection (°)	6.80 to 30.57
Total reflections	8605
Reflection with (F>4$\sigma_{(F)}$)	3093
R$_{(F)}^{a}$(%)	3.38
WR$_2^{b}$(%)	8.78

$$R_{(F)}{}^a = \sum \|F_O| - |F_C\| / \sum |F_O|$$

$$WR_2 = \left[\frac{\Sigma \left[w\left(|F_O|^2 - |F_C|^2\right)\right]^2}{\Sigma \left[w\left(|F_O|^2\right)\right]^2} \right]^{\frac{1}{2}}$$

Table 2.

Atoms	x	y	z	$U_{éq}$	Occ
Se1	0.6605(2)	0.69234(8)	0.77785(9)	0.00783(8)	1
Se3	0.16097(2)	0.81096(8)	0.67578(9)	0.00820(8)	1
Se2/Cu2	0.4991(2)	1.00230(13)	0.72682(6)	0.01156(6)	0.63/0.37
Cu1	0.44385(8)	1.13914(6)	0.97711(3)	0.01349(3)	1
O1	0.3674(7)	1.2885(9)	0.9006(5)	0.030(2)	1
O2	0.3643(9)	1.2826(9)	1.0580(5)	0.0174(5)	1
O3	0.2292(8)	0.9552(7)	0.7268(5)	0.0131(4)	1
O4	0.7410(9)	0.5457(7)	0.7274(5)	0.0138(4)	1
O5	0.5576(9)	0.7955(7)	0.7096(4)	0.0084(1)	1
O6	0.0611(3)	0.7160(8)	0.7447(5)	0.0169(5)	1
O7	0.4737(1)	0.6070(8)	0.8188(4)	0.0155(4)	1
O8	-0.0378(9)	0.8841(9)	0.6305(5)	0.0190(5)	1
O9	0.7275(7)	1.2328(6)	0.9728(1)	0.0371(5)	1
Cl1	0.0815(5)	1.0791(9)	0.9747(6)	0.185(4)	1
Cl2	0.5125(5)	0.9726(4)	0.88370(8)	0.0204(5)	1
Cl3	0.5120(5)	0.9717(4)	1.07037(9)	0.0256(6)	1
H1	0.438(5)	1.300(5)	0.859(2)	0.05	1
H3	0.264(6)	1.232(6)	1.042(3)	0.007	1
H4	0.376(10)	1.255(8)	1.1065(5)	0.007	1
H2	0.256(6)	1.325(4)	0.887(4)	0.05	1
H7	-0.090(10)	0.939(7)	0.667(3)	0.004	1
H6	0.667(6)	1.217(2)	0.9289(9)	0.026	1
H5	0.837(5)	1.186(8)	0.966(4)	0.026	1
H8	0.456(5)	0.655(9)	0.863(3)	0.02	1

Table 3.

Anisotropic displacement parameters (in $10^{-3}Å^2$)	U11	U22	U33	U23	U13	U12
Se1	0.002(2)	0.006(2)	0.015(3)	-0.002(2)	-0.001(2)	0.0017(14)
Cu1	0.0167(17)	0.0099(15)	0.0140(16)	-0.002(4)	-0.001(4)	0.0010(12)
Se2/Cu2	0.0048(15)	0.0057(15)	0.0240(18)	-0.008(11)	0.0004(10)	-0.0003(9)
Se3	0.006(3)	0.007(2)	0.012(3)	-0.002(2)	0.002(2)	0.0002(1)
O1	0.05(3)	0.02(5)	0.01(5)	-0.002(1)	-0.001(1)	0.01(2)
O2	0.008(17)	0.02(2)	0.02(3)	0.002(9)	0.005(16)	0.005(16)
O3	0.001(9)	0.011(10)	0.026(3)	-0.011(9)	0.001(9)	-0.003(7)
O4	0.005(9)	0.014(11)	0.022(5)	-0.002(9)	-0.004(10)	0.001(8)

O5	0.010(10)	0.005(8)	0.015(2)	-0.003(8)	-0.005(9)	0.008(7)
O6	0.027(15)	0.001(9)	0.019(14)	0.003(9)	0.002(1)	0.0001(1)
O7	0.025(14)	0.018(12)	0.011(12)	-0.006(9)	0.006(10)	-0.013(11)
O8	0.001(8)	0.030(13)	0.018(14)	-0.001(10)	-0.007(8)	0.002(8)
O9	0.028(9)	0.029(9)	0.07(4)	0.018(18)	0.014(14)	-0.009(7)
Cl1	0.027(3)	0.0141(8)	0.099(5)	0.069(19)	0.08(3)	0.06(2)
Cl2	0.028(5)	0.019(4)	0.016(4)	0.001(4)	-0.002(4)	0.004(3)
Cl3	0.041(6)	0.015(4)	0.019(5)	0.003(4)	-0.001(5)	0.006(4)

Table 4.

a: SeO_3 polyhedron

Se1-O4 = 1.70(5)	O5 – Se1 – O7 = 102(2)
Se1-O5 = 1.70(5)	O5 – Se1 – O4 = 102(2)
Se1-O7 = 1.71(5)	O7 – Se1 – O4 = 98(2)
Se3-O3 = 1.67(4)	O3 – Se3 – O6 = 98(3)
Se3-O6 = 1.66(6)	O3 – Se3 – O8 = 101(3)
Se3-O8 = 1.77(5)	O6 – Se3 – O8 = 100(2)

b: Cu/SeO_4Cl_2

Cu2/Se2 – O3 = 1.98(4)	O4$^{(b)}$ – Cu2/Se2 – O6$^{(a)}$ = 91(2)
Cu2$^{(c)}$ /Se2$^{(c)}$ – O4$^{(b)}$ = 1.91(4)	O4$^{(b)}$ – Cu2/Se2 – O3 = 179(3)
Cu2/Se2 – O5 = 1.94(4)	O6$^{(a)}$ – Cu2/Se2 – O3 = 90(2)
Cu2$^{(d)}$ /Se2$^{(d)}$ – O6$^{(a)}$ = 2.01(5)	O4$^{(b)}$ – Cu2/Se2 – O5 = 89(2)
Cu2 /Se2 – Cl2 = 2.77(2)	O6$^{(a)}$ – Cu2/Se2 – O5 = 180(4)
Cu2 /Se2 – Cl3$^{(e)}$ = 2.80(2)	O3 – Cu2/Se2 – O5 = 90.1(2)
	Cl2 – Cu2/Se2 – O6$^{(a)}$ = 89.52(8)
	O3 – Cu2/Se2 – Cl3$^{(e)}$ = 89.11(5)
	Cl2 – Cu2/Se2 – O3 = 91.1(4)
	Cl2 – Cu2/Se2 – O4$^{(b)}$ = 89.83(3)
	O5 – Cu2/Se2 – Cl2 = 94.18(7)

c: $CuCl_3(H_2O)$ octahedron

Cu1 – Cl1 = 2.66 (8)	O1 – Cu1 – O2 = 88.1(3)
Cu1 – Cl2 = 2.30 (2)	O1 – Cu1 – Cl3 = 176(2)
Cu1 – Cl3 = 2.30(2)	O1 – Cu1 – Cl2 = 90.9(2)
Cu1 – O1 = 1.99(7)	O2 – Cu1 – Cl2 = 176.1(5)
Cu1 – O2 = 2.02(6)	O2 – Cu1 – Cl1 = 83(2)
Cu1 – O9 = 2.21(3)	Cl3 – Cu1 – Cl2 = 92.2(3)
	Cl3 – Cu1 – Cl1 = 94.1(3)

Symmetry code: ^{a} –x+1/2,y+1/2,z; ^{b} –x+3/2,y+1/2,z; ^{c} –x+3/2,y -1/2,z ; ^{d} –x+1/2,y-1/2,z ; ^{e} –x+1,-y+2,z+1/2

Table 5.

O(d) -H….X	O(d) –H (Å)	H….X (Å)	<DHX (°)	O(d) ..A (Å)
O1-H1... O6[(a)]	1.157	1.842	147.8	2.887
O2-H3... Cl1	0.931	2.222	162.56	3.122
O2-H3... O8[(f)]	0.931	2.449	123.84	3.067
O2-H4…O5[(g)]	0.956	1.875	177.42	2.83
O1-H2...Cl2[(a)]	0.986	2.393	139.55	3.208
O8-H7... O4[(a)]	0.901	1.807	167.16	2.693
O9-H6... O1	0.9	2.315	125.26	2.928
O9-H6... Cl2	0.9	2.586	129.04	3.23
O9-H5...Cl1[(h)]	0.9	2.01	168.89	2.899
O7-H8...Cl1[(d)]	0.894	1.994	148.9	2.797

Symmetry codes: [a] –x+1/2,y+1/2,z ; [f] -x,-y+1,z+1/2 ; [g] -x+1,-y+2,z+1/2 ; [h] x+1,y,z ; [d] -x+1/2,y-1/2,z

.